

RESEARCH

CLear: An Adaptive Continual Learning Framework for Regression Tasks

Yujang He^{*} and Bernhard Sick

Abstract

Catastrophic forgetting means that a trained neural network model gradually forgets the previously learned tasks when retrained on new tasks. Overcoming the forgetting problem is a major problem in machine learning. Numerous continual learning algorithms are very successful in incremental classification tasks, where new labels appear frequently. However, there is currently no research that addresses the catastrophic forgetting problem in regression tasks as far as we know. This problem has emerged as one of the primary constraints in some applications, such as renewable energy forecasts. This article clarifies the problem-related definitions and proposes a new methodological framework that can forecast regression task targets and update itself by continual learning. The framework consists of forecasting neural networks and buffers, which store newly collected data from a data stream in an application. Changes in the probability distribution of the data stream will be identified by the framework and learned sequentially. The framework is called CLear (Continual Learning for Regression Tasks), where components can be flexibly customized for a specific application scenario. We design two sets of experiments to evaluate the CLear framework concerning fitting error (training), prediction error (test), and forgetting ratio. The first one is based on an artificial time series to explore how hyperparameters affect the CLear framework. The second one is designed with data collected from European wind farms to evaluate the performance of the CLear framework in a real-world application. The experimental results demonstrate that the CLear framework can efficiently accumulate knowledge in the data stream and improve the prediction accuracy. The article concludes with further research issues arising from requirements to extend the framework.

Keywords: Continual learning; Renewable energy forecasts; Regression tasks; Deep neural networks

Introduction

In the late 1980s, McCloskey and Cohen [1] and Ratcliff [2] observed a phenomenon where the well-learned knowledge of connectionist models is erased by new knowledge under specific conditions when the models learn new tasks successively. It is referred to as Catastrophic Forgetting or Catastrophic Interference. The challenge is supposed to be a general problem existing in different neural networks, e.g., back-propagation neural networks and unsupervised neural networks. The weights of a hidden layer in neural networks can be expressed as a vector $W = [w_1, w_2, \dots, w_N]$ with N values. Some weights have a significant influence on more than one task. For example, w_1, w_2, w_3 are important for task 1 and w_1, w_4, w_5 are important for task 2. In this case, the overlapped weight w_1 could be

adjusted during learning task 2 sequentially, which is one of the main reasons for Catastrophic Forgetting.

Overcoming the forgetting problem is a crucial step in implementing real intelligence. Models require plasticity for learning and integrating new knowledge as well as stability for consolidating what models have learned previously. Excessive plasticity can cause the acquired knowledge to be erased during learning new tasks. Moreover, sequentially learning tasks can become more challenging due to extreme stability. It is the so-called stability-plasticity dilemma [3].

Many researchers have proposed continual learning (CL) algorithms to solve the problem, such as in [4, 5, 6]. A three-way categorization for the most common CL strategies is described in [6]: (1) regularization strategies, (2) rehearsal strategies, and (3) architectural strategies. Similarly, CL strategies are grouped as (1) prior-focused approaches, (2) likelihood-focused approaches, and (3) dynamic architectures in [7]. These categorizations standardize

^{*}Correspondence: yujang.he@uni-kassel.de

Intelligent Embedded Systems (IES) Group, University of Kassel,
Wilhelmshöher Allee 71 - 73, Kassel, Germany

terminologies and outline a distinct research direction for the CL community. CL algorithms have been proven successful in supervised learning and reinforcement learning to train several tasks sequentially without forgetting the acquired ones. Application scenarios cover handwriting recognition [8, 9, 10], image classification [5], sequentially learning to play games in a reinforcement learning setting [4] and much more.

To our best knowledge, some of the standard CL benchmarks are the reconstructions of well-known datasets, such as permuted MNIST [11, 12], where the CL tasks are obtained by scrambling the pixel positions in the MNIST dataset [13]. Moreover, some datasets are explicitly generated to evaluating CL algorithms, for example, CORE50 [14] for continuous object recognition.

Most of the past research focused mainly on classification tasks rather than regression tasks, where the Catastrophic Forgetting problem usually occurs. For example, establishing regional smart grids requires power generation and consumption forecasts. In [15] and [16], neural networks are used to forecast renewable energy generation with weather prediction data. Note that the probability distribution of weather data usually changes periodically. In this situation, training neural networks has to be delayed until sufficient data is collected. Otherwise, the networks could be overfitted to the limited training dataset. Furthermore, unseen situations, e.g., the extreme weather conditions, updating/repairing/aging of generators, and climate changes, can be called special events. The neural networks have to update themselves by continually learning these situations when they appear in the application. Besides, power consumption regarding a household or a factory is also easily affected by unpredictable things, such as purchasing new equipment or hiring more employees. These factors can change the obtained mapping between inputs and outputs. Under the condition where historical data may be private, unrecorded, or too cumbersome to be retrained, the trained models have to learn new knowledge and consolidate the previously-stored internal representations without the help of old data.

In this article, we thus propose a framework called CLear (Continual Learning for Regression Tasks). The CLear framework consists of neural networks for prediction and buffers for storing new data. New data collected from a data stream is labeled by calculating an error between the predictions and the true values and then comparing the error to a dynamically preset threshold. If the error is larger than the threshold, the data is labeled as novelty and stored in a finite novelty buffer, or else stored as familiarity in an infinite familiarity buffer. When the novelty buffer is full,

updating will be triggered. The network will be retrained on the dataset in the novelty buffer using CL. The retrained network will then be tested on the familiarity dataset to evaluate how much old knowledge is retained. The threshold will be adjusted depending on how well the retrained network performs on the dataset of both buffers after updating. Afterward, the buffers will be emptied, and updating will be repeated until the novelty buffer is filled again.

The remainder of the article starts with a literature review on CL algorithms and applications. Then we outline the proposed framework's fundamental structure and give an insight into the experimental details. Furthermore, we discuss the experimental results. Finally, we conclude the article with an outlook for future research.

Related work

This section gives a brief overview of the recent academic literature regarding approaches and experimental setups designed for CL applications.

In both [6] and [7], CL algorithms are categorized into three groups in a similar way. Firstly, the prior-focused approaches (also regularization strategies) denote that the posterior probability of N tasks is a sum of the likelihood of the N th task and the posterior probability of the first $N - 1$ tasks. As a regularization, the posterior probability of the first $N - 1$ tasks is added in the loss function to avoid changing the weights that are important for previous tasks. Well-known prior-focused algorithms include Elastic Weight Consolidation (EWC) [4], Synaptic Intelligence (SI) [5], Variational Continual Learning [8]. In [9], a generalization of EWC++ and SI was proposed, which is referred to as the RWalk algorithm.

Secondly, likelihood-focused approaches (also rehearsal strategies) require a subset of randomly selected samples from the original dataset of the previous $N - 1$ tasks, or a dataset generated by a generative network that has learned the tasks, see in [17, 7, 10].

Thirdly, dynamic architectures (also architectural strategies) enable neural networks to learn CL tasks sequentially by adjusting the architecture of the networks for specific applications. Progressive Networks, Learning Without Forgetting (LWF), and Less-Forgetting Learning have been introduced in [18, 19, 20], respectively.

The above algorithms have been evaluated in multi-task scenarios with the reshaped versions of famous datasets, e.g., MNIST and CIFAR-10/CIFAR-100. In these scenarios, a model learns a new, isolated task in a sequence while it remembers how to solve the learned tasks. However, no class overlaps among the different tasks. For example, in [5] the MNIST dataset

is split into five tasks, one of which contains two labels (two digits). The model can classify data correctly into one of the two labels, only if the information regarding the current task is given. In this case, the model learns how to solve a series of discrete tasks rather than accumulate information for addressing incremental problems. The experimental setups and the datasets mislead a comparison among the CL algorithms. Lomonaco et al. [14] create CORE50 specifically for single-incremental-task scenarios, which can be seen as a test benchmark for continuous objective recognition. Similarly, the iCubWorld benchmark [21] is designed for robotic vision challenges, where comparison among various CL approaches is feasible.

All of the above experiments address only classification problems. In [22], He et al. propose two CL application scenarios for establishing regional smart grids: the task-domain incremental scenario and the data-domain incremental scenario. The scenarios are applicable for forecasting power, including renewable energy generation and power consumption in the middle-/low-voltage grid. Moreover, performances of four CL algorithms (EWC, Online-EWC, SI, and LWF) are evaluated concerning accuracy, forgetting ratio, and training time in the two scenarios. However, prior knowledge about new tasks is given in their experimental setup, which means that models know when new tasks will occur without novelty detection. Therefore, this setup is incompatible with the real world.

In [23], Farquhar et al. conclude that an inappropriate experimental design could misrepresent performances of the well-known CL approaches. Therefore, they suggest five requirements for evaluating CL algorithms and demonstrate their necessities. The five requirements are: (1) cross-task resemblances; (2) shared output head; (3) no test-time assumed task labels; (4) no unconstrained retraining on old tasks; and (5) more than two tasks.

These suggestions are worth being considered in our experimental setup and inspire us to design the CLear framework. (1) Most novelties are from the probability distribution changing periodically over time. The dataset of every full novelty buffer can be viewed as a new task that resembles the previous tasks. (2) The neural network outputs the power value prediction, and the new tasks will not change the architecture of the network. (3) Besides, the prior knowledge regarding the new tasks is unknown in the application. Updating is triggered automatically only when the finite novelty buffer is filled in our experimental setup. (4) Considering that privacy laws might prohibit the long-term storage of historical datasets, we retrain the neural network only on the dataset newly collected in applications and delete it after updating. (5) More

tasks will appear as the probability distribution and the mapping between inputs and outputs change over time

Energy forecasts using deep neural networks

Deep neural networks are a kind of machine learning inspired by biological neural networks to model non-linear prediction on high dimensional data. Compared with traditional high dimensional data reduction techniques, such as principal component analysis (PCA), the multiple deep layers of a neural network can extract representations efficiently from massive data to provide predictive performance gains.

The rest of this section provides a brief interpretation of deep neural networks from a Bayesian perspective. Moreover, this section illustrates the probability distribution changes in the experimental dataset over time and clarifies how the CLear framework works in a general energy forecasting workflow.

Deep neural networks

Deep neural networks can predict outputs Y with given high-dimensional inputs X . The goal of training is to find a mapping between X and Y . A general deep neural network consists of a series of hidden layers, which can be formulated as:

$$Z_l^\theta = f_l(\theta_l^T Z_{l-1}) \quad (1)$$

with an input vector Z_{l-1} from the $l-1$ th layer, where $Z_0 = X$. Here θ_l^T represents a transposed weight matrix of the l th layer, and the f_l is an activation function. A prediction $\hat{Y}(X)$ of the deep neural network is then

$$\hat{Y}(X) = f_L(\theta_L^T \dots \theta_2^T f_1(\theta_1^T X)), \quad (2)$$

where L is the number of layers.

From a probabilistic perspective, the likelihood function of the output Y with the given X and θ is $P(Y|\hat{Y}(X)) = P(Y|X, \theta)$. Alternatively, in another way to understand, the output Y is generated by the probability model $P(Y|X, \theta)$. Optimizing a regression model can be generally defined as minimizing the function

$$L(Y, \hat{Y}(X)) = \|Y - \hat{Y}(X)\|_2^2 = -\log P(Y|X, \theta) \quad (3)$$

to find the optimal parameters. To avoid overfitting during training, prior knowledge about the parameters can be added to the loss function, namely

$$L(Y, \hat{Y}(X)) = -\log P(Y|X, \theta) - \log P(\theta|\lambda). \quad (4)$$

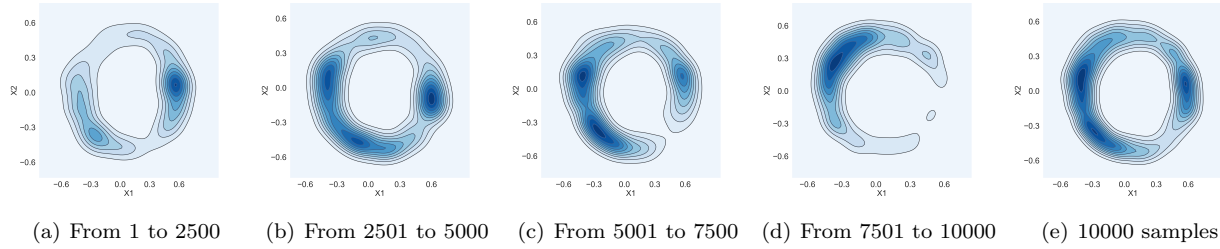


Figure 1 Distributions of the inputs change over time. We split 10000 samples into four sections sequentially over time, each of which has 2500 samples, and visualize their two-dimensional distributions from (a) to (d). (e) illustrates the distribution of the same 10000 samples. Both axes in the sub-figures, X_1 and X_2 , indicate the first two principal components extracted from seven-dimensional weather features, respectively.

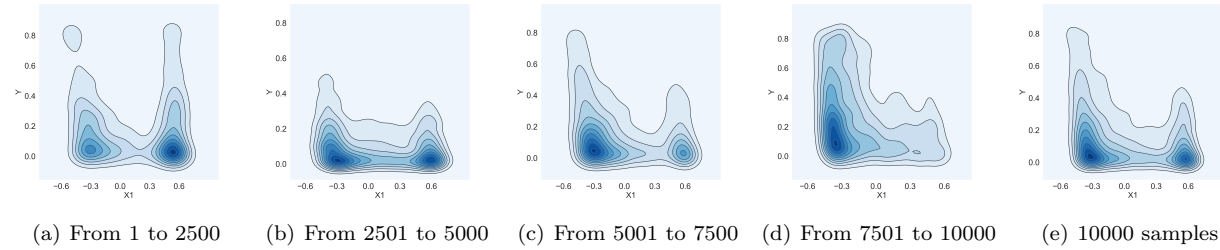


Figure 2 Distributions of the input and the output change over time. We split 10000 samples into four sections sequentially over time, each of which has 2500 samples, and visualize their two-dimensional distributions from (a) to (d). (e) illustrates the distribution of the same 10000 samples. Both axes in the sub-figures, X_1 and Y , indicate the first principal component extracted from seven-dimensional weather features using PCA and the power value, respectively.

Probabilistically, a trained deep neural network is a maximum posterior estimator with a regularization

$$\begin{aligned} P(\theta|D) &\propto P(Y|X, \theta)P(\theta|\lambda) \\ &\propto \exp(-\log P(Y|X, \theta) - \log P(\theta|\lambda)). \end{aligned} \quad (5)$$

Note that the posterior estimation is relevant to the given dataset. If the statistic property of the dataset's distribution changes, such as the mean or the variance, the optimal parameters also need to be adjusted.

Change in probability distribution

A learning task can be described as a joint probability distribution of observations $P(X, Y)$. In our experimental setup, X and Y represent the meteorological features as inputs and the power measurements as outputs, respectively. Some meteorological features, such as temperature, wind direction, are yearly periodic. Thus the probability distributions about the features could change over time. Also, renewable energy generation, such as solar energy and wind energy, depends on meteorological conditions. Therefore, the mapping between the features and the power measurements needs to be updated to the new distribution. Mathematically,

the change can be expressed as follows:

$$\exists t_0 \neq t_1 : P(X_{t_0}, Y_{t_0}) \neq P(X_{t_1}, Y_{t_1}), \quad (6)$$

where t_0 and t_1 denote two time points. The following formula,

$$P(X, Y) = P(Y|X)P(X), \quad (7)$$

demonstrates that $P(X, Y)$ is affected by the change in the probability distribution of the inputs and the obtained mapping.

Figs. 1 and 2 illustrate the change regarding $P(X)$ and $P(Y|X)$ based on a European wind farm dataset. A sample of the dataset contains seven-dimensional meteorological features and a univariate power value. The first two principal components are extracted from seven features using PCA and labeled as X_1 and X_2 . 64.19% of variance are explained by the two components. We split 10000 samples from the dataset into four sections sequentially over time, each of which has 2500 samples. The distribution of each section regarding the X_1 and the X_2 is plotted in Fig. 1. Similarly, the distributions of four sections regarding the X_1 and

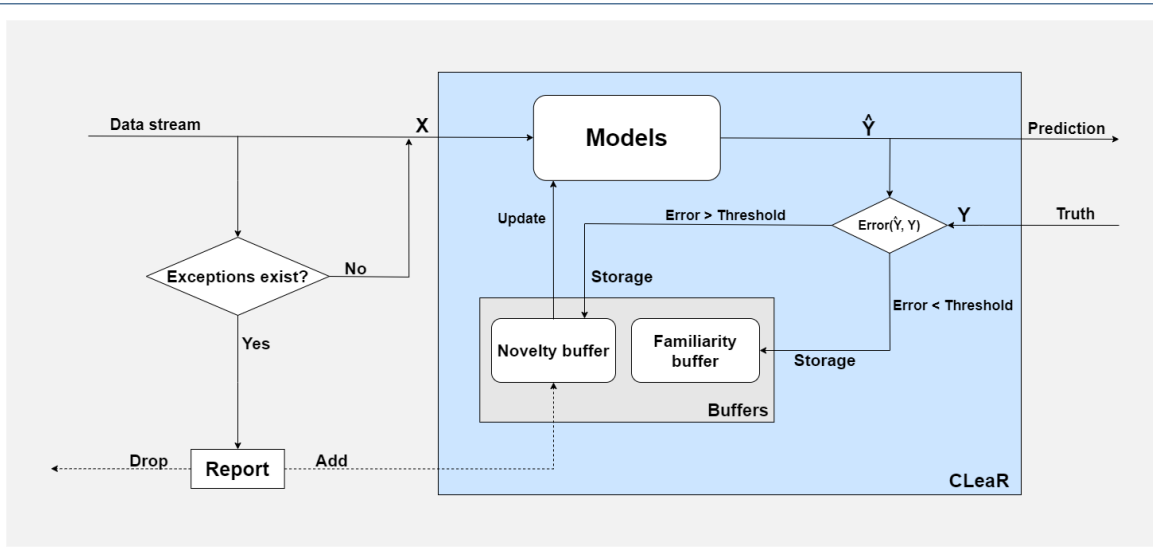


Figure 3 A general workflow of energy forecasts comprises four phases: (1) reporting exceptions, (2) predicting targets, (3) storing data, and (4) updating models.

the power Y are shown in Fig. 2. The distributions of $P(X1, X2)$ and $P(X1, Y)$ with the same 10000 samples are plotted in Fig. 1(e) and Fig. 2(e) in comparison to other sub-figures.

The two-dimensional probability distribution of $P(X1, X2)$ with 10000 samples shows a circular shape, as in Fig. 1(e). From Fig. 1(a) to 1(d), the center of the contour line regarding each section moves clockwise along the circle. This movement illustrates the periodic change in the $P(X)$ over time. Similarly, we can observe that the center of the distribution $P(Y|X)$ moves from right to left over time, as shown in Fig. 2.

Combined with Eq. 6 and the observations, we conclude that the periodic change exists in the dataset. The model needs to be updated spontaneously in applications if it was pre-trained only on a limited dataset.

Energy forecasting workflow

We suggest that a general energy forecasting workflow should comprise four phases: (1) reporting exceptions, (2) predicting targets, (3) storing data, and (4) updating models, as shown in Fig. 3.

Exceptions have to be identified first as the data arrives. If it exists in the data stream, the exceptions need to be reported and processed manually. Here we define that an exception deviating from the expected model is an outcome from an unknown process. For example, wind power generators are automatically shut down for protection under extreme weather conditions, such as typhoons or storms. Although the dataset used here has been cleaned in the preprocessing phase, these

exceptions might appear in applications. Labeling and learning exceptions are one of the research focuses in the field of active learning, which is beyond the scope of this article. It can be further researched in the future.

The CLear framework contains the models for prediction and the buffers for storage. Once the measurements Y are available, the corresponding data is labeled and stored into the two buffers depending on the preset threshold and the error. We choose the Mean Square Error (MSE) here for supervised regression tasks, but the method can be customized in other scenarios, e.g., probabilistic forecasts. The data in the novelty buffer includes the change of probability distribution detected in the data stream. It is used for retraining the models when the update is triggered. The data in the familiarity buffer has information that the models are familiar with. It can be used for testing whether the models still retain the old knowledge after updating. Updating models can be considered as accumulations of knowledge for improving prediction accuracy.

CLear

The details of the CLear framework will be explained through the instance used in our experiments, as shown in Fig. 4. In this instance, the block **Models** contains an autoencoder and a fully-connected neural network for detecting the changes of the distribution $P(X)$ and $P(Y|X)$ and for forecasting power values. Data is labeled as novelty and familiarity by comparing the MSE to the threshold. Besides, we adopt Online-EWC to update the models and adjust the threshold

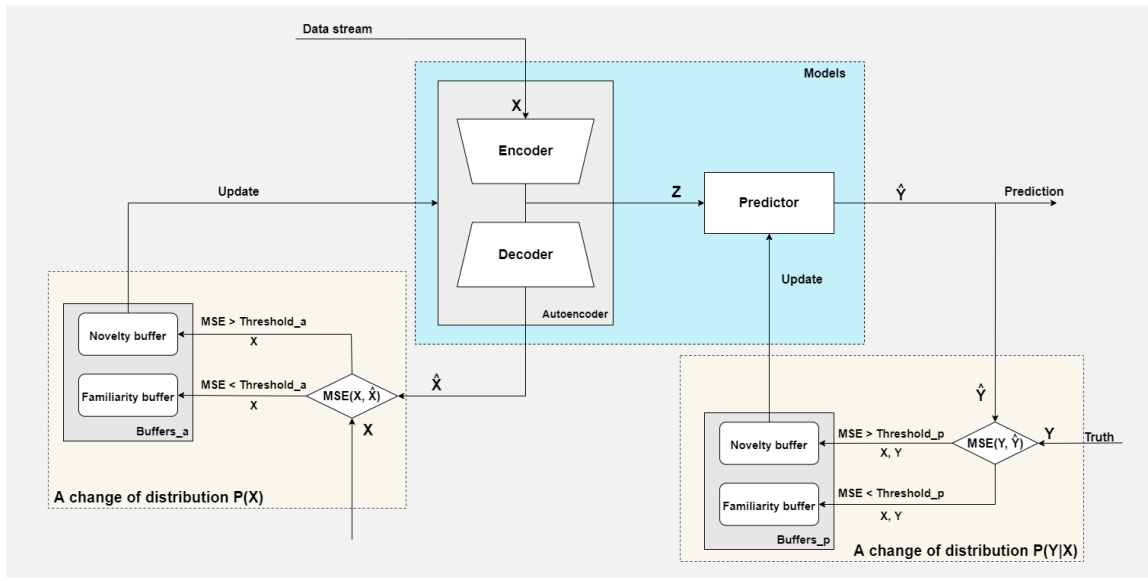


Figure 4 The CLear instance contains an autoencoder and a fully-connected neural network in the block **Models**. The $MSE(X, \hat{X})$ is compared to **Threshold_a** to detect the change of $P(X)$, and the $MSE(Y, \hat{Y})$ is compared to **Threshold_p** to detect the change of $P(Y|X)$. The novelty buffer in **Buffers_a** is for updating the autoencoder and the novelty buffer in **Buffers_p** is for updating the predictor. Models are evaluated with the data in the familiarity buffer.

dynamically after each update. We suggest that the components of the CLear framework should be selected flexibly depending on the specific application scenario.

Models

An autoencoder is a neural network that usually consists of two symmetric parts with a bottleneck between them. In an undercomplete autoencoder, the bottleneck has a smaller dimension than the input layer, which helps to extract latent representations Z from the input. An autoencoder can reconstruct the input at the output, rather than simply copy the input [24]. The encoder and the decoder can be formulated $Z = f_{\theta}(X)$ and $\hat{X} = g_{\phi}(Z)$, where θ and ϕ are the parameter vectors. The optimization goal is to minimize the loss function

$$L(X, \phi, \theta) = MSE(X, g_{\phi}(f_{\theta}(X))), \quad (8)$$

by penalizing the reconstruction being different from the input. The change of distribution $P(X)$, as shown in Fig. 1, can be detected by the reconstruction error of the autoencoder.

At the next step, the extracted representation Z is fed into the predictor. As explained in Eqs. 3 and 4, optimizing the network in the general supervised setting is to minimize the MSE. Thus true measurement Y is required. The predictor, a fully-connected neural network, can be replaced by other networks, e.g., LSTM.

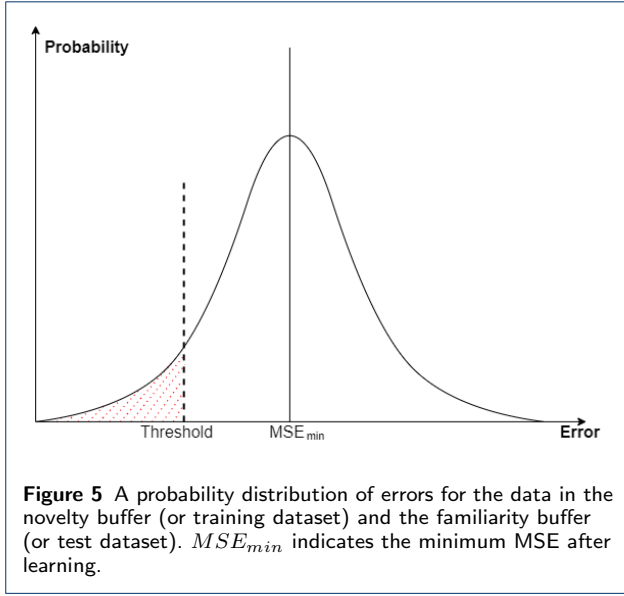
Also, we can drop the predictor under the situation where only the reconstruction is needed.

Buffers

Every neural network that needs to be updated during its application owns a finite novelty buffer and an infinite familiarity buffer. When true target values are provided, MSE can be used as a criterion to be compared to the preset threshold. The samples with a small MSE are stored in the familiarity buffer because the trained network has learned to cope with them before. The samples with a large MSE are stored in the novelty buffer. The network needs to be retrained based on these novelties to learn new knowledge. After updating, a validation error can be calculated using the familiarities to estimate whether the network can still retain the old knowledge acquired previously. How to deal with a poor update result remains an open question and needs to be further researched. We empty both buffers after finishing an update.

Threshold

The value of the threshold determines how new samples are classified. The smaller the threshold, the more samples are likely to be labeled as novelties, where more well-learned knowledge will be re-learned, thus leading to unnecessary updates. A huger threshold could cause inefficient updates because too many novelties are missing. We suggest that the threshold value



should be adjusted dynamically depending on the training results.

Fig. 5 illustrates a distribution of errors for all samples after learning. MSE_{min} refers to the minimum MSE obtained by minimizing a loss function, which can also be viewed as the mean of the distribution. The distribution has a lower mean and a lower variance indicating the model learns better on the given dataset. In this article, we adjust the threshold by

$$Threshold = \alpha \times MSE_{min}, \text{ with } \alpha > 0, \quad (9)$$

where α is a fixed threshold factor and the MSE_{min} is re-estimated after each update.

Update

The updating method and the trigger condition play a crucial role in the CLear framework. As mentioned in Section of related work, retraining on old tasks should be constrained due to reasons, such as privacy protection or data storage overhead. Therefore, we adopt Online-EWC, which penalizes the loss when the overlapped important weights are changed during learning new tasks. We adapt the notation given in [25] to explain EWC and Online-EWC using the notation of the CLear framework.

EWC

The goal of EWC is to approximate Bayesian posteriors over model parameters given tasks. In the CLear, data is always split according to two kinds of tasks, the known task (T_k) and the unknown task (T_u). T_k refers to what the neural network has already learned. The corresponding dataset D_k was stored in the novelty

and the familiarity buffers during the $T - 1$ th update. Note that novelties in D_k have already been learned before the T th update. Thus we classify it to the known task. Comparably, T_u refers to what the network will learn at the T th update. The corresponding D_u refers only to the dataset stored in the novelty buffer for triggering the T th update. Chronologically, the $T - 1$ th update occurs before the T th update. The posterior after learning T_u can be written as:

$$\log P(\theta|D_u, D_k) = \log P(D_u|\theta) + \log P(\theta|D_k) - \log P(D_u|D_k), \quad (10)$$

where θ indicates the adjustable parameters of the model.

The term, $\log P(D_u|\theta)$, is generally tractable through minimizing an MSE loss with respect to θ and the dataset D_u . Assumed that the trained network can perform very well on the known task T_k , namely, we have gotten the optimal parameters θ_k^* , which makes the gradient of $-\log P(\theta|D_k)$ with respect to θ equal to 0. Therefore, the $-\log P(\theta|D_k)$ can be estimated using 2nd order Taylor series around θ_k^* :

$$-\log P(\theta|D_k) \approx \frac{1}{2}(\theta - \theta_k^*)^T H(\theta_k^*)(\theta - \theta_k^*), \quad (11)$$

where $H(\theta_k^*)$ is the Hessian of $-\log P(\theta|D_k)$ with respect to θ , evaluated at the optima θ_k^* . Furthermore, we can approximate the Hessian as:

$$H(\theta_k^*) \approx N_k \cdot F(\theta_k^*) + H_{prior}(\theta_k^*), \quad (12)$$

where N_k is the number of samples in D_k , and $F(\theta_k^*)$ is the empirical Fisher information matrix on the known dataset D_k , and $H_{prior}(\theta_k^*)$ is the Hessian of the prior with respect to θ . EWC estimates the Fisher information matrix in a high-dimensional space as a diagonal matrix, where the non-diagonal elements are zero [4]. The diagonal Fisher information values are denoted by F_k^i concerning the i th parameter in the network. Thus the formula of EWC is expressed as:

$$\theta_{k,T}^* = \argmin_{\theta} \{ -\log P(D_{u,T}|\theta) + \frac{1}{2} \sum_i \left(\sum_{t=1}^{T-1} \lambda_t F_{k,t}^i + \lambda_{prior} \right) (\theta^i - \theta_{k,T-1}^{*,i})^2 \}, \quad (13)$$

where the update has been done $T - 1$ times. $D_{u,T}$ is the dataset stored in the novelty buffer for the unknown task at the T th update. $F_{k,t}^i$ is the diagonal Fisher information with respect to the parameter i , estimated by the dataset $D_{k,t}$ stored in both buffers after the T th update. $\theta_{k,T-1}^{*,i}$ is the optimal parameter i learned from the dataset $D_{k,T-1}$ after the $T - 1$ th

update. λ_t and λ_{prior} are hyperparameters for EWC. Note that all of the diagonal Fisher information $F_{k,t}$ in Eq. 13, obtained after every update, must be stored.

Online-EWC

The penalties in EWC can be replaced by one Gaussian approximation to the whole posterior of all previous tasks, as proven in [25]. Based on the derivation, Online-EWC is proposed in [26]. The regularization is formulated as:

$$R_{Online-EWC} = \frac{1}{2} \sum_i \lambda \tilde{F}_{k,T-1}^i (\theta^i - \theta_{k,T-1}^{*,i})^2. \quad (14)$$

where $\tilde{F}_{k,T}^i = \gamma \tilde{F}_{k,T-1}^i + F_{k,T}^i$ and $\tilde{F}_{k,1}^i = F_{k,1}^i$. γ is a hyperparameter governing the contribution of previous tasks and not larger than 1. Therefore, $\tilde{F}_{k,T-1}^i$ contains diagonal Fisher information of all updates which precede the T th update.

By contrast with EWC, Online-EWC requires less space to store diagonal Fisher information and optima of each previous task. Another similar algorithm is EWC++ introduced in [9], where the diagonal Fisher information is defined as: $\tilde{F}_{k,T-1}^i = \alpha \tilde{F}_{k,T-1}^i + (1 - \alpha) F_{k,T}^i$ with $0 < \alpha < 1$. In our experiments, Online-EWC is selected to update the CLear framework.

Trigger condition

The trigger condition for the model update is another customizable parameter. Our design is that the update will be triggered when the finite novelty buffer is filled. The smaller the size of this novelty buffer, the more easily this buffer gets full. At the same time, more updates will result in increasing computational overhead. Moreover, note that the hyperparameter γ of Online-EWC is not larger than 1, which causes a gradual decay of the previous Fisher information when the number of updates increases. If the size is too large, updating the network will be delayed until the buffer is full. The delay also results in that the threshold can not be adjusted in time.

Experiments

In this section, two sets of experiments are performed. An unsupervised artificial dataset is generated for experiment 1, where we analyze the effects of two hyperparameters of the CLear, the novelty buffer size and the threshold factor. We implement experiment 2 on a supervised dataset regarding the wind power generation measured in 10 European wind farms [27]. In this experiment, we evaluate the performance of the CLear regarding prediction accuracy and continual updating in wind energy prediction applications. Both experiments will evaluate three metrics: fitting error, prediction accuracy, and forgetting ratio. The remainder

of the section will introduce the datasets, the experimental setup, the evaluation criteria, and analyze the results.

Dataset

Artificial dataset is a seven-dimensional periodic unsupervised dataset sampled from a time-dependent Gaussian distribution, see as follows:

$$\begin{aligned} x_i(t) &\sim N(\text{mean}_i(t), \text{var}_i(t)), \\ \text{mean}_i(t) &= A_m \times \left| \sin\left(\frac{\pi \times (t + p_i)}{T}\right) \right|, \\ \text{var}_i(t) &= A_v \times \left| \sin\left(\frac{\pi \times (t + p_i)}{T}\right) \right|, \\ p_i &\sim N(0, 1), \end{aligned} \quad (15)$$

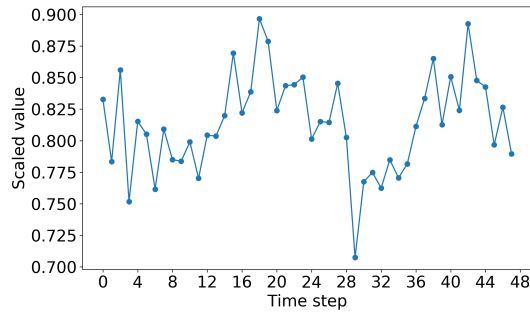
where $x_i(t)$ denotes the i_{th} -dimension univariate at time step t . The mean and variance are sampled from an absolute value of a sinusoidal function with a period T and a phase p_i . The phase p_i is randomly generated with a standard normal distribution. Hyperparameters A_m and A_v refer to the amplitude of the sinusoid.

The i th dimensional sequence of the dataset is a sum of two sequences with different periods, i.e. $x_i(t) = x_i^d(t) + x_i^y(t)$. The period T_d of $x_i^d(t)$ is 24 to simulate the fluctuation in a day (24 hours). Also, the period T_y of $x_i^y(t)$ is 8760 for the periodic changes over a year (8760 hours). Examples of the sequences are displayed in Fig. 6.

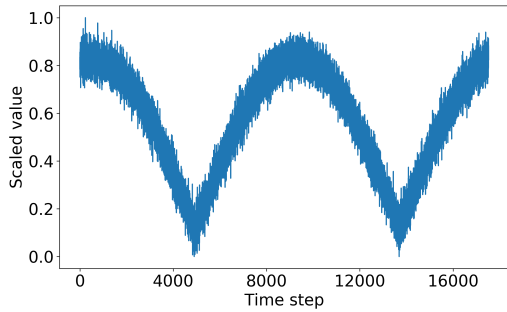
Wind power dataset [27] contains seven meteorological features and hourly averaged wind power generation data measured from European wind farms for two years in a row. The features are 24-hour-ahead meteorological forecasts using the European Centre for Medium-Range Weather Forecasts model, including (1) wind speed in 100m height, (2) wind speed in 10m height, (3) wind direction (zonal) in 100m height, (4) wind direction (meridional) in 100m height, (5) air pressure, (6) air temperature, and (7) humidity.

The power generation time series are normalized by the respective rated capacity of the wind farm for easy, scale-free comparison. All features are normalized to the range between 0 and 1. When no power has been generated longer than 24 hours, time points are removed in the pre-processing. The dropped time points can be viewed as exceptions that need to be processed manually in real-world applications.

The wind power dataset is available on the department homepage [27] or by contacting the corresponding author. Researchers can re-implement our experiments with the dataset.



(a) $x_i^d(t)$ over 48 hours (2 days)



(b) $x_i^y(t)$ over 17520 hours (2 years)

Figure 6 The two figures illustrate the fluctuation of i_{th} dimension sequence over 48 hours (2 days) and 17520 hours (2 years), respectively

Experimental setup

The artificial dataset and the wind power data are split into three phases: a warm-up phase, an update phase, and an evaluation phase. In the warm-up phase, the model is pre-trained on the first 1000 samples, which contain only partial information that can not exactly describe the real sample space. The model monitors a data stream with the following 10000 samples in the update phase, which simulates a theoretically infinite data stream in a real application scenario. Assuming that 10000 samples can provide enough information to describe the real distribution of samples, because 10000 samples span 10000 hours. The model detects the change of the distribution and will be re-trained based on the buffers if updating is triggered. The updated model is finally evaluated in the evaluation phase with the following 1000 samples.

We implement these three CLear instances to compare their performances in experiments:

- **Instance_A**: Its models are trained on the warm-up dataset in supervised learning and evaluated in the third phase. The experimental results can

reflect the disadvantages due to the lack of samples. Instance_A is viewed as a **baseline**.

- **Instance_B**: Its models are pre-trained in the warm-up phase, as Instance_A. Then the models will be updated in the update phase by using **fine-tuning**. Fine-tuning allows the pre-trained models to learn a new dataset, which they were not originally trained on, by slightly adjusting all unfrozen parameters. The re-training process is monitored by early stopping with 30 of patience to avoid overfitting. It means the re-training process will stop if the loss is no longer decreasing in 30 epochs. The optimal models are the ones with the lowest loss before stopping. Similarly, the updated Instance_B will be evaluated in the evaluation phase after the update phase.
- **Instance_C**: is similar to Instance_B, but uses **Online-EWC** without being monitored by early stopping for updating.

Two sets of experiments are conducted on the artificial dataset and the wind power dataset, respectively.

- **Experiment 1** is based on the artificial dataset to analyze the performance of the CLear framework with respect to two hyperparameters, the novelty buffer size and the threshold factor. In this unsupervised experiment, only Instance_C with an autoencoder is involved. It aims to extract latent representations and reconstruct the inputs. The novelty buffer size ranges from 400 to 1800, with a step size of 200. The threshold factor ranges from 0.5 to 1.4, with a step size of 0.15.
- **Experiment 2** aims at evaluating the three CLear instances in the real-world application of wind power generation forecast. Every instance consists of an autoencoder and a deep neural network as a predictor, as proposed in Fig. 4. Grid search parameters and a training setup are shown in Tables 1 and 2.

We empirically select the same architecture of models in the three instances for a fair comparison, as listed in Table 3. For experiment 1, the Instance_C contains only the encoder and the decoder, namely from the encoder input layer to the decoder output layer in Table 3. Note that dropout layers are used in the autoencoder to avoid overfitting.

Metrics

The three instances are evaluated in terms of fitting error, prediction error, and forgetting ratio.

Fitting error indicates how well the instance fits all seen samples after the update phase. Because a CLear instance is updated by mini-batch data every time, some batches may lead it to a local minimum during

Table 1 A dictionary for grid search parameters. The parameter λ_a is the lambda value for the autoencoder, and λ_p is for the predictor. Latent size is the dimension of the bottleneck in the autoencoder.

Hyperparameter	Dictionary
Dropout	{0, 0.005}
Novelty buffer size	{512, 1024}
Latent size	{4, 5}
γ	{0.7, 0.8, 0.9}
λ_a	{200}
λ_p	{600, 800}

Table 2 The Training setting of the experiment 2. The parameter epoch_a denotes the number of iterations for training the autoencoder and epoch_p for training the predictor. The batch size is the size of a mini-batch. Phase 1 and phase 2 indicate the warm-up phase and the update phase, respectively.

Hyperparameter	Reference figure
Optimizer	Adam
Epochs _a in phase 1	256
Epochs _p in phase 1	256
Batch size in phase 1	32
Epochs _a in phase 2	128
Epochs _p in phase 2	256
Batch size in phase 2	16

Table 3 Architecture parameters of the three instances in experiment 1 and 2. Dropout layers are used in the encoder layers with a dropout value selected by grid search. Latent_size refers to the bottleneck dimension in an autoencoder. The slope parameter of the LeakyReLU is set to 0.05.

Layer	Size	Activation
Encoder-Input	7	None
Encoder-1	7×32	LeakyReLU
Encoder-2	32×16	LeakyReLU
Encoder-3	16×8	LeakyReLU
Decoder-1	8×16	LeakyReLU
Decoder-2	16×32	LeakyReLU
Decoder-3	32×7	LeakyReLU
Decoder-Output	7	None
DNN-1	Latent_size×96	Tanh
DNN-2	96×64	Tanh
DNN-3	64×32	Tanh
DNN-4	32×16	Tanh
DNN-5	16×8	Tanh
DNN-Output	8×1	None

the update process. Eventually, the instance fits only a specific subset, rather than all of the seen data. Such effects are measured by calculating MSE on the 11000 samples, 1000 of which are from the warm-up phase and the rest 10000 are from the update phase. Therefore, a lower fitting error reflects that more knowledge is finally accumulated.

Prediction error reflects the ability of CLear instances to predict unseen data. It is calculated with 1000 samples in the evaluation phase. The overfitting problem often exists due to neural networks' powerful learning ability, where a test error is much larger than a training error. Regularization techniques, such as dropout and early stopping, are used to avoid overfitting during training. The prediction error can tell us

whether the instance has already fallen into a local optimum after several updates. Also, the comparison between Instance_A and Instance_C in experiment 2 shows how important accumulating data and updating model are for improving prediction accuracy, especially under the condition with limited pre-training dataset.

Forgetting ratio is a metric proposed in [22] to measure how much previous knowledge a model forgets after learning new tasks. They compared the forgetting ratio to average test error and demonstrated that the forgetting ratio could reflect the severity of the forgetting problem. The formula is

$$\text{forgetting ratio} = \frac{\max(0, L_{\text{warm-up}}^2 - L_{\text{warm-up}}^1)}{L_{\text{warm-up}}^1}, \quad (16)$$

where $L_{\text{warm-up}}^1$ indicates the MSE on the warm-up dataset at the end of the warm-up phase and $L_{\text{warm-up}}^2$ indicates the error on the same dataset at the end of the update phase. $\max(x_1, x_2)$ returns the larger one of either x_1 or x_2 . The increment of the error for the same task describes the model's forgetfulness after learning new tasks. The comparison is performed only between Instance_B and Instance_C in experiment 2, because Instance_A is not updated in the update phase.

Results of the experiment 1

In experiment 1, we explore the influence of hyperparameters on the performance of the CLear. Fifty-six groups of experiments with different hyperparameters are repeated 20 times with different random seeds for initialization to reduce the stochastic influence during training. In Figs. 7 and 8, the fitting error and prediction error are plotted logarithmically with a base of 2 for a good visualization. The yellow stars connected by the yellow dashed line in the figures indicate the mean results of 20 repeated experiments under each set of parameter values. The black diamonds above the boxes and the black lines inside the boxes indicate the outliers and the medians, respectively.

The similar features in Figs. 7 and 8 are that the yellow dashed lines show a W-shaped trend, i.e., low and fluctuated in the middle and high on both sides. Besides, in the figures regarding fitting error and prediction error, the length of the box in the middle is smaller than on both sides. We suppose that the CLear instance is more robust when the novelty buffer size is 1200 and the threshold factor is 0.95, because the variance of the results is the smallest in the experiment.

We can also observe that the CLear instance is also robust to the forgetting problem, except when the size of novelty buffer is beneath 800 in Fig. 8(c). It is empirically explainable that a smaller novelty buffer size

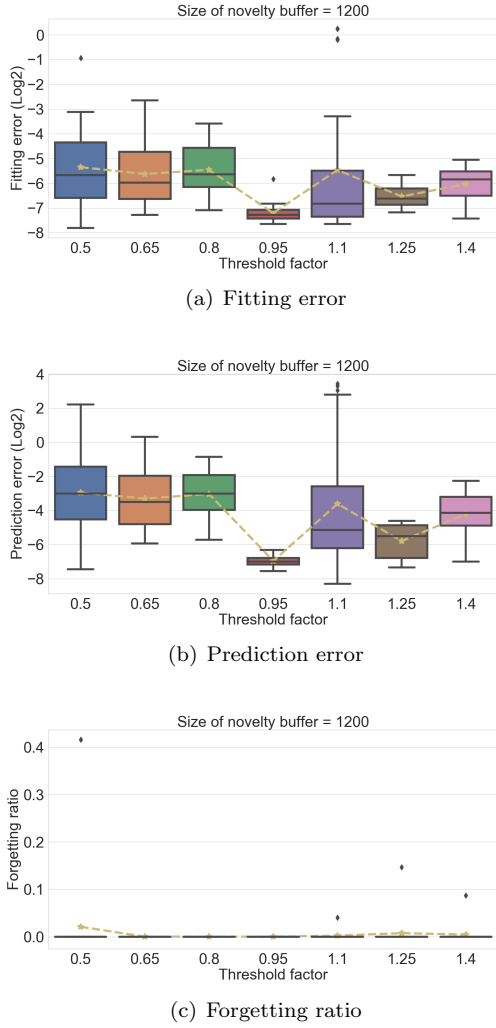


Figure 7 The influence of the threshold factor with the novelty buffer size fixed to 1200. Experiments are repeated 20 times with different initialization under the same setting. Black diamonds above boxes denote outliers, and the black lines in boxes denote the medians. Yellow stars connected by the dashed line indicate the mean values of 20 repeats.

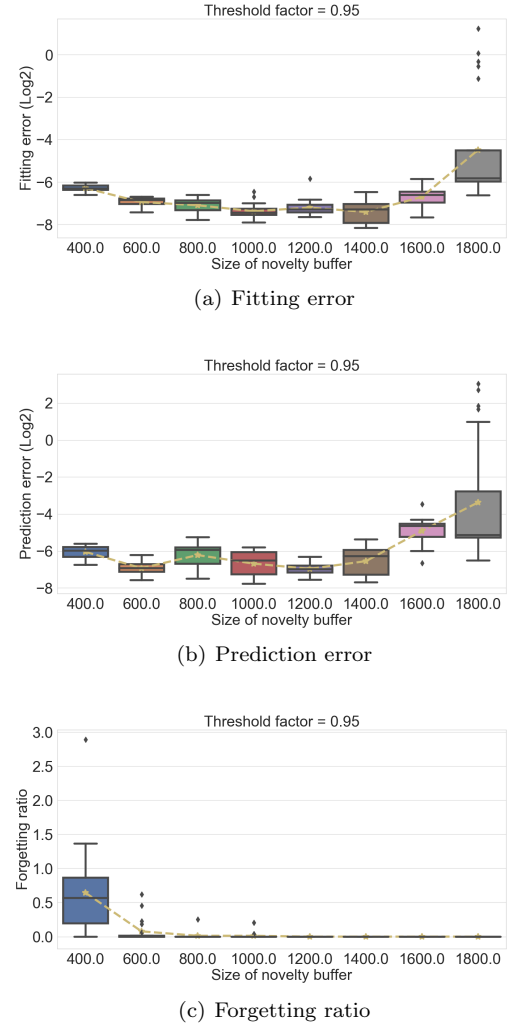


Figure 8 The influence of novelty buffer size with the threshold factor fixed to 0.95. Experiments are repeated 20 times with different initialization under the same setting. Black diamonds above boxes denote outliers, and the black lines in boxes denote the medians. Yellow stars connected by the dashed line indicate the mean values of 20 repeats.

triggers the update more frequently since the novelty buffer is filled quickly. As we mentioned, the hyperparameter γ of Online-EWC is usually smaller than 1. The diagonal Fisher information estimated on the previous tasks will be gradually forgotten as more and more updates are triggered.

Due to space limitations, here we only show the experimental results with one set of hyperparameters. The patterns observed in the other results could be similar but not identical. Interested readers can contact us to get the 56 sets of results and the artificial dataset we used.

Results of the experiment 2

In experiment 2, we evaluate the three CLeaR instances' performance based on 10 European wind farms.

Tables 4 and 5 record the fitting errors for 11000 samples regarding the weather-to-weather data (the output of the autoencoder) and the weather-to-power data (the output of the predictor), respectively. WF is the abbreviation of the wind farm. The values on the last row of the tables are the mean results for the 10 wind farms. In Table 4, the fitting error of autoencoders in Instance B_{ae} and Instance C_{ae} are much smaller than that in Instance A_{ae} , where ae refers to the

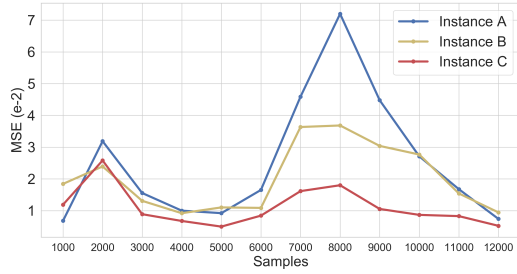


Figure 9 Errors of the three instances about one wind farm. Each point refers to the mean error over 1000 samples.

autoencoder in a CLear instance. However, the difference in Table 5 is that the fitting error of Instance_B is highest.

The error results of predicting wind power are listed in Table 6, where Instance_C outperforms the other two instances. Fig. 9 illustrates the errors of the three instances over the 12000 weather-to-power samples from one wind farm. The errors are calculated after the update phase. We split the samples into 12 sections, and each point in Fig. 9 refers to the MSE for 1000 samples. Points correspond to the fitting error at coordinates from 1000 to 11000 and the prediction error at 12000.

Compared to the blue and the yellow lines, the red line is less volatile. Moreover, we can observe that the lines start to rise at the coordinate of 5000 and drop back to the original level at the end. On the one hand, it reflects that the periodic changes might lead to the fluctuated curves and influence the mapping between weather and power generation. On the other hand, in Tables 5, 6, and Fig 9, where Instance_C outperforms the other instances, it proves that updating is necessary to predict a changing data stream, especially when the model is trained only on a limited dataset.

Table 7 presents the the forgetting ratio values between Instance_B and Instance_C, calculated after the

Table 4 The fitting error of the **autoencoders** in the three CLear instances.

Dataset	Fitting error (e-2)		
	Instance _A _{ae}	Instance _B _{ae}	Instance _C _{ae}
WF 1	2.098	0.369	0.502
WF 2	2.068	0.348	0.440
WF 3	2.292	0.423	0.513
WF 4	2.669	0.988	0.863
WF 5	1.421	0.516	0.471
WF 6	2.456	1.054	0.761
WF 7	2.129	0.647	0.931
WF 8	2.149	0.434	0.662
WF 9	2.370	0.773	0.793
WF 10	1.996	0.678	0.411
Mean	2.165	0.623	0.635

Table 5 The fitting error of the **predictor** in the three CLear instances.

Dataset	Fitting error (e-2)		
	Instance _A	Instance _B	Instance _C
WF 1	4.864	3.468	2.304
WF 2	2.695	2.120	1.167
WF 3	3.517	9.172	1.769
WF 4	4.867	5.457	3.682
WF 5	10.347	12.989	6.931
WF 6	9.593	6.089	4.225
WF 7	0.867	0.838	0.677
WF 8	8.042	5.656	3.451
WF 9	4.713	5.511	3.060
WF 10	1.875	3.117	1.025
Mean	5.138	5.442	2.829

Table 6 The prediction error of the **predictor** in three CLear instances.

Dataset	Prediction error (e-2)		
	Instance _A	Instance _B	Instance _C
WF 1	2.415	2.332	1.822
WF 2	0.740	0.945	0.522
WF 3	2.370	5.369	1.208
WF 4	2.124	1.643	2.223
WF 5	13.864	5.672	5.560
WF 6	8.612	8.017	4.368
WF 7	0.965	0.729	0.587
WF 8	6.129	4.969	2.927
WF 9	2.544	4.562	1.808
WF 10	1.383	3.009	0.741
Mean	4.115	3.725	2.177

Table 7 The forgetting ratio of Instance_B and Instance_C.

Dataset	Forgetting ratio			
	Instance _B _{ae}	Instance _C _{ae}	Instance _B	Instance _C
WF 1	1.474	0.727	1.955	0.994
WF 2	0.018	0.140	1.707	0.745
WF 3	1.205	1.489	6.170	0.421
WF 4	2.817	2.407	3.371	0.785
WF 5	0.000	0.000	7.617	2.296
WF 6	0.945	0.237	0.969	0.046
WF 7	0.574	1.552	1.768	1.253
WF 8	0.588	1.585	5.716	2.999
WF 9	1.463	0.848	3.470	1.463
WF 10	4.937	2.726	2.754	0.609
Mean	1.402	1.171	3.550	1.161

update phase. As can be seen, Instance_C outperforms Instance_B here, for both the weather-to-weather task and the weather to-power task.

Conclusion

In the article, the CLear only broadly describes the prototype structure of the framework. The framework still needs to be improved in future research. For example, although the cleaned exception is not considered, it is necessary to define and process such exceptions in a real application. Also, we only use MSE to calculate the difference between predictions and measurements. However, this method might not work when the values are unavailable in unsupervised settings. Therefore, we suggest estimating the uncertainty of new predictions,

for example, using Monte Carlo dropout [28]. If the uncertainty is over a threshold, the data can be labeled as novelties. Also, hyperparameters are found by grid search in the context of the current design. It is worth researching whether hyperparameters can be found by transferring relevant knowledge from a similar task dataset. Furthermore, we suppose that Online-EWC can be replaced by (or combined with) other CL algorithms to improve the framework. It will be one of our future research focuses.

To be summarized, we expect that the framework could be designed as a modular tool like LEGO toys. Each component of the framework is flexible and can be added, removed, replaced, or expanded. It should be possible for researchers and users to adapt the model to a specific application scenario for achieving their desired goals.

Abbreviations

CL: Continual Learning; MSE: Mean Square Error; EWC: Elastic Weight Consolidation; SI: Synaptic Intelligence; LWF: Learning Without Forgetting; Online-EWC: Online Elastic Weight Consolidation; PCA: Principal Component Analysis;

Funding

Not applicable

Availability of data and materials

The datasets generated and analyzed during the current study are available from www.uni-kassel.de/eecs/de/fachgebiete/ies/downloads.html or the corresponding author on reasonable request.

Competing interests

The authors declare that they have no competing interests.

Author's contributions

YH wrote the majority of the manuscript and was responsible for implementing the CLear and experiments. BS suggested the artificial data and the first experiment and was responsible for double-checking the manuscript. All authors read and approved the final manuscript.

Acknowledgements

Thanks to the IES colleagues at the University of Kassel, whose reviews and comments have helped to improve the manuscript.

References

- McCloskey, M., Cohen, N.J.: Catastrophic interference in connectionist networks: The sequential learning problem **24**, 109–165 (1989)
- Ratcliff, R.: Connectionist models of recognition memory: constraints imposed by learning and forgetting functions. *Psychological review* **97**(2), 285 (1990)
- Mermillod, M., Bugaiska, A., Bonin, P.: The stability-plasticity dilemma: Investigating the continuum from catastrophic forgetting to age-limited learning effects. *Frontiers in psychology* **4**, 504 (2013)
- Kirkpatrick, J., Pascanu, R., Rabinowitz, N., Veness, J., Desjardins, G., Rusu, A.A., Milan, K., Quan, J., Ramalho, T., Grabska-Barwinska, A., et al.: Overcoming catastrophic forgetting in neural networks. *Proceedings of the national academy of sciences* **114**(13), 3521–3526 (2017)
- Zenke, F., Poole, B., Ganguli, S.: Continual learning through synaptic intelligence. *Proceedings of machine learning research* **70**, 3987 (2017)
- Maltoni, D., Lomonaco, V.: Continuous learning in single-incremental-task scenarios. *Neural Networks* **116**, 56–73 (2019)
- Farquhar, S., Gal, Y.: A unifying bayesian view of continual learning. *arXiv preprint arXiv:1902.06494* (2019)
- Nguyen, C.V., Li, Y., Bui, T.D., Turner, R.E.: Variational continual learning. *arXiv preprint arXiv:1710.10628* (2017)
- Chaudhry, A., Dokania, P.K., Ajanthan, T., Torr, P.H.: Riemannian walk for incremental learning: Understanding forgetting and intransigence. In: *Proceedings of the European Conference on Computer Vision (ECCV)*, pp. 532–547 (2018)
- van de Ven, G.M., Tolias, A.S.: Generative replay with feedback connections as a general strategy for continual learning. *arXiv preprint arXiv:1809.10635* (2018)
- Goodfellow, I.J., Mirza, M., Xiao, D., Courville, A., Bengio, Y.: An empirical investigation of catastrophic forgetting in gradient-based neural networks. *arXiv preprint arXiv:1312.6211* (2013)
- Srivastava, R.K., Masci, J., Kazerooni, S., Gomez, F., Schmidhuber, J.: Compete to compute. In: *Advances in Neural Information Processing Systems*, pp. 2310–2318 (2013)
- LeCun, Y., Cortes, C., Burges, C.: Mnist handwritten digit database. ATT Labs [Online]. Available: <http://yann.lecun.com/exdb/mnist> 2 (2010)
- Lomonaco, V., Maltoni, D.: Core50: a new dataset and benchmark for continuous object recognition. *arXiv preprint arXiv:1705.03550* (2017)
- Gensler, A., Henze, J., Sick, B., Raabe, N.: Deep learning for solar power forecasting — an approach using autoencoder and lstm neural networks. In: *2016 IEEE International Conference on Systems, Man, and Cybernetics (SMC)*, pp. 002858–002865 (2016). doi:[10.1109/SMC.2016.7844673](https://doi.org/10.1109/SMC.2016.7844673)
- He, Y., Henze, J., Sick, B.: Forecasting power grid states for regional energy markets with deep neural networks. In: *2020 International Joint Conference on Neural Networks (IJCNN)*, pp. 1–8 (2020). IEEE
- Shin, H., Lee, J.K., Kim, J., Kim, J.: Continual learning with deep generative replay. In: *Advances in Neural Information Processing Systems*, pp. 2990–2999 (2017)
- Rusu, A.A., Rabinowitz, N.C., Desjardins, G., Soyer, H., Kirkpatrick, J., Kavukcuoglu, K., Pascanu, R., Hadsell, R.: Progressive neural networks. *arXiv preprint arXiv:1606.04671* (2016)
- Li, Z., Hoiem, D.: Learning without forgetting. *IEEE Transactions on Pattern Analysis and Machine Intelligence* **40**(12), 2935–2947 (2017)
- Jung, H., Ju, J., Jung, M., Kim, J.: Less-forgetting learning in deep neural networks. *arXiv preprint arXiv:1607.00122* (2016)
- Pasquale, G., Ciliberto, C., Rosasco, L., Natale, L.: Object identification from few examples by improving the invariance of a deep convolutional neural network. In: *2016 IEEE/RSJ International Conference on Intelligent Robots and Systems (IROS)*, pp. 4904–4911 (2016). IEEE
- He, Y., Henze, J., Sick, B.: Continuous Learning of Deep Neural Networks to Improve Forecasts for Regional Energy Markets. (in press) (2020)
- Farquhar, S., Gal, Y.: Towards robust evaluations of continual learning. *arXiv preprint arXiv:1805.09733* (2018)
- Goodfellow, I., Bengio, Y., Courville, A.: *Deep Learning*. MIT Press. <http://www.deeplearningbook.org>
- Huszár, F.: On quadratic penalties in elastic weight consolidation. *arXiv preprint arXiv:1712.03847* (2017)
- Schwarz, J., Luketina, J., Czarnecki, W.M., Grabska-Barwinska, A., Teh, Y.W., Pascanu, R., Hadsell, R.: Progress & compress: A scalable framework for continual learning. *arXiv preprint arXiv:1805.06370* (2018)
- Gensler, A.: EuropeWindFarm Data Set (2016). <https://www.uni-kassel.de/eecs/de/fachgebiete/ies/downloads.html>
- Gal, Y., Ghahramani, Z.: Dropout as a bayesian approximation: Representing model uncertainty in deep learning. In: *International Conference on Machine Learning*, pp. 1050–1059 (2016)